

Recommended snapshot length for acoustic point-transect surveys of intermittently available Cuvier's beaked whales

Jay Barlow,^{1,a)} Jennifer S. Trickey,² Gregory S. Schorr,³ Shannon Rankin,¹ and Jeffrey E. Moore¹

¹Marine Mammal and Turtle Division, National Oceanic and Atmospheric Administration, National Marine Fisheries Service, Southwest Fisheries Science Center, 8901 La Jolla Shores Drive, La Jolla, California 92037, USA

²Ocean Associates Inc., Arlington, Virginia 22207, USA

³Marine Ecology and Telemetry Research, Seabeck, Washington 98380, USA

ABSTRACT:

Acoustic point-transect distance-sampling surveys have recently been used to estimate the density of beaked whales. Typically, the fraction of short time “snapshots” with detected beaked whales is used in this calculation. Beaked whale echolocation pulses are only intermittently available, which may affect the best choice of snapshot length. The effect of snapshot length on density estimation for Cuvier's beaked whale (*Ziphius cavirostris*) is investigated by sub-setting continuous recordings from drifting hydrophones deployed off southern and central California. Snapshot lengths from 20 s to 20 min are superimposed on the time series of detected beaked whale echolocation pulses, and the components of the density estimation equation are estimated for each snapshot length. The fraction of snapshots with detections, the effective area surveyed, and the snapshot detection probability all increase with snapshot length. Due to compensatory changes in these three components, density estimates show very little dependence on snapshot length. Within the range we examined, 1–2 min snapshots are recommended to avoid the potential bias caused by animal movement during the snapshot period and to maximize the sample size for estimating the effective area surveyed. <https://doi.org/10.1121/10.0005108>

(Received 13 November 2020; revised 26 April 2021; accepted 7 May 2021; published online 3 June 2021)

[Editor: Aaron M. Thode]

Pages: 3830–3840

I. INTRODUCTION

Point transects are a distance-sampling survey method for estimating the density and abundance of animals from points that are selected to representatively cover a study area (Buckland, 2006). Typically, point-transect surveys are conducted from multiple randomly selected points, and estimated densities are averaged to estimate population abundance for a defined study area. These types of surveys are commonly used for bird species in heavily wooded areas where line-transect surveys are impractical (Lee and Marsden, 2008). However, because animals are frequently moving and the observation point is not, the time period of sampling is a critical parameter in designing a point-transect survey. The bias in density estimates caused by random animal movement is small for line-transect surveys if the survey speed is more than twice the animal's speed but is always a concern for stationary point-transect surveys (Buckland, 2006; Glennie *et al.*, 2020). In choosing the appropriate sampling period for point-transect distance-sampling surveys, there is an inherent trade-off between meeting two assumptions: that all individuals at zero distance are detected (which leads to a negative bias in density if not met) and that animals are stationary (which leads to a positive bias if not met and if movement is random with respect to the observation point). Longer sampling periods help to

ensure the first assumption is met but increase the likelihood of violating the second assumption, and vice versa. For point-transect surveys, Buckland (2006) recommended using a “snapshot” approach, i.e., using a short time window during which animal movement can be assumed to be insignificant. Lee and Marsden (2008) examined this trade-off in selecting snapshot lengths for Philippine forest bird surveys. They found the optimal snapshot window ranged from 4 to 10 min based on the behavioral characteristics of different bird groups. Although alternative approaches exist, such as cue-counting and modeling of animal movement (Hildebrand *et al.*, 2015; Glennie *et al.*, 2020), the snapshot approach is more appropriate in many instances.

There is growing interest in applying point-transect methods in acoustic surveys of cetaceans (Marques *et al.*, 2013). Hildebrand *et al.* (2015) and Barlow *et al.* (2021) developed snapshot-based point-transect methods to estimate the density of beaked whales from detections of their echolocation signals and used a snapshot length of 5 and 1 min, respectively. Cuvier's beaked whales (*Ziphius cavirostris*) are excellent candidates for acoustic surveys because their acoustic behavior is consistent and predictable. They typically produce echolocation pulses only during foraging dives when they are deeper than ~500 m (Tyack *et al.*, 2006; Warren *et al.*, 2017). During foraging, they regularly produce echolocation pulses every 0.33–0.40 s (Zimmer *et al.*, 2005; Baumann-Pickering *et al.*, 2013). These pulses are loud, with an estimated source level of 224

^{a)}Electronic mail: jay.barlow@noaa.gov, ORCID: 0000-0001-7862-855X.

$\text{dB}_{\text{p-p}}$ re $1 \mu\text{Pa}$ at 1 m (Gassmann *et al.*, 2015). On-axis pulses are detectable to ranges of at least 4 km (Zimmer *et al.*, 2008; Barlow *et al.*, 2018). However, this species also presents some challenges. On average, Cuvier’s beaked whales make only one deep foraging dive (with a typical duration of 58–67 min) every 121–191 min (Tyack *et al.*, 2006; Schorr *et al.*, 2014; Barlow *et al.*, 2020) during both day and night. Because they make echolocation pulses only during the deep portion of deep foraging dives, the fraction of their total time spent echolocating is only 20%–28% (Barlow *et al.*, 2013; Barlow *et al.*, 2020). Furthermore, because their echolocation signals are highly directional (Zimmer *et al.*, 2008), they are likely to be detectable only when whales are oriented toward a hydrophone. Therefore, Cuvier’s beaked whales are only intermittently available for acoustic detection.

Barlow *et al.* (2021) used acoustic data from a drifting recording system to estimate the population density of Cuvier’s beaked whales. That system, also used for this study, records signals from two hydrophones configured as a vertical hydrophone array ~ 100 m below the surface. With this configuration, the vertical angle to a signal source can be estimated from the time-difference-of-arrival of the signal on the two hydrophones. Barlow *et al.* (2021) estimated the density of beaked whale individuals, D , in the vicinity of a point using the formula

$$\hat{D} = \frac{n \cdot \hat{s}}{k \cdot \hat{v} \cdot \hat{\lambda}}, \tag{1}$$

where n is the number of snapshot time periods with detections of Cuvier’s beaked whale groups, k is the total number of snapshots, \hat{v} is the estimated effective area surveyed, $\hat{\lambda}$ is the estimated probability a group is available to be detected within a snapshot, and \hat{s} is the estimated mean group size. This approach assumes that only one group is detected during a snapshot. The fraction of snapshots with detections, F , is estimated as

$$F = \frac{n}{k}. \tag{2}$$

Barlow *et al.* (2021) estimated snapshot availability, $\hat{\lambda}$, as the fraction of a dive cycle during which animals are actively foraging and producing regular echolocation pulses (instantaneous availability), corrected for snapshot length (1 min) (see Sec. IID). They estimate \hat{v} from the distribution of vertical bearing angles to echolocating beaked whales and the distribution of depths at which beaked whales echolocate using a maximum simulated likelihood approach.

Here, we use empirical observations from continuous recordings on drifting hydrophone arrays to study the effects of snapshot length on estimates of F , \hat{v} , and $\hat{\lambda}$ and on the resulting estimates of D . We also use simulations to explore the expected effect of snapshot length on F given observed levels of intermittent availability. Based on our results, we recommend snapshot lengths for future studies.

II. METHODS

A. Empirical studies

Drifting acoustic spar buoy recorders (DASBRs) were deployed off central and southern California in 2016–2019 (Fig. 1 and Table I) to study the density and distribution of Cuvier’s beaked whales (*Ziphius cavirostris*). Each DASBR consisted of a digital recording system [SM3M (Wildlife Acoustics, Maynard, MA) or Soundtrap ST4300 (Ocean Instruments, Auckland, New Zealand)], which recorded acoustic signals from a vertical array of two hydrophones suspended 100–150 m below a surface buoy (Keating *et al.*, 2018; Simonis *et al.*, 2020). Two-minute acoustic WAV files were recorded continuously at a sampling rate of 256 kHz (SM3M recorder) and 288 or 576 kHz (ST4300 recorder). A “drift” is considered to be the deployment and retrieval of a single instrument. Two drifts were conducted in September 2016 (offshore of central and southern California, over the abyssal plain), six drifts were conducted in January 2018 (all in the San Nicolas Basin), and six drifts were conducted in June 2019 (three in the Santa Cruz Basin, two in the San Nicolas Basin, and one in the Catalina Basin) (Fig. 1). The drifts in 2016 were by far the longest (19–20 days). Drifts from 2018 were shorter (9.2–28 h) than in 2019 (~ 48 h). Both drifts in 2016 and one drift in 2019 used SM3M recorders, and all other drifts used ST4300 recorders (Table I). The 2016 data were from a larger study that included 30 drifts (Keating *et al.*, 2018); however, most of the 2016 drifts used duty-cycled recordings, and we only include drifts with continuous recordings in this study. Due to difference in drift durations and beaked whale density,

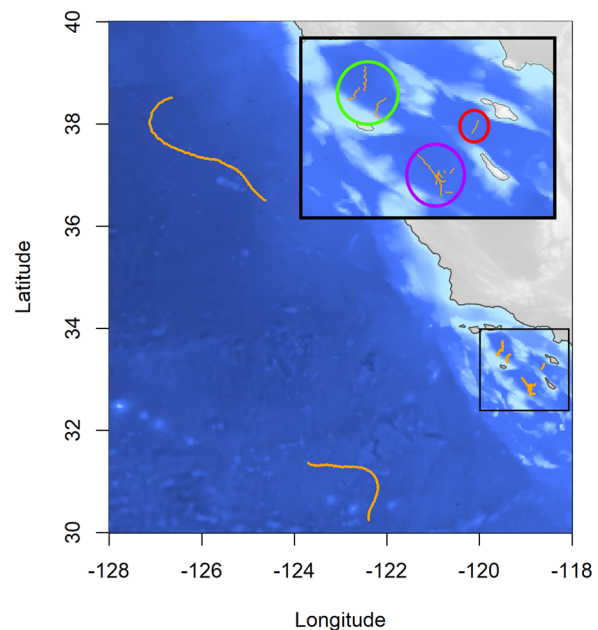


FIG. 1. (Color online) DASBR drifts off central and southern California are illustrated with orange lines. Drifts in the deep basins of southern California (black rectangle) are also shown in the inset with circles denoting drifts in the Santa Cruz Basin (green), the San Nicolas Basin (magenta), and the Catalina Basin (red). West longitudes are negative and north latitudes are positive.

TABLE I. Summary of deployment information and acoustic detections of Cuvier’s beaked whales for 14 DASBR drifts off central and southern California. Two drifts were over the abyssal plain, and the remainder were in deep basins off southern California [San Nicolas Basin (SNB), Santa Cruz Basin (SCB), and Catalina Basin (CB)]. Minimum group size is the mean of minimum estimates of all dives detected during a drift. Coordinated universal times (UTC) are given for the start and end of recordings.

Year	Drift	Location	Recorder	Start date/time (UTC)	End date/time (UTC)	Recording duration (h)	No. of dives	Dive detection rate (h ⁻¹)	% minutes with echolocation	Minimum group size
2016	7	Abyssal north	SM3M	8/25/2016 03:31	9/13/2016 03:27	455.9	37	0.081	1.3	1.38
2016	17	Abyssal south	SM3M	9/1/2016 21:55	9/21/2016 17:11	475.3	19	0.040	0.4	1.37
2018	1	SNB	ST4300	1/4/2018 09:24	1/4/2018 18:39	9.3	2	0.216	0.7	1.50
2018	2	SNB	ST4300	1/5/2018 11:04	1/6/2018 13:20	26.3	11	0.419	11.5	1.58
2018	3	SNB	ST4300	1/11/2018 14:40	1/12/2018 08:00	17.3	3	0.173	8.0	2.67
2018	4	SNB	ST4300	1/12/2018 15:04	1/13/2018 08:32	17.5	7	0.401	17.5	2.57
2018	5	SNB	ST4300	1/13/2018 08:58	1/14/2018 12:40	27.7	13	0.469	14.9	1.67
2018	6	SNB	ST4300	1/14/2018 09:57	1/15/2018 07:52	21.9	7	0.319	15.9	2.50
2019	1	SCB	ST4300	6/1/2019 06:53	6/3/2019 06:23	47.5	6	0.126	3.5	2.00
2019	2	SCB	ST4300	6/1/2019 08:12	6/3/2019 07:35	47.4	11	0.232	6.5	1.75
2019	3	SCB	SM3M	6/1/2019 10:16	6/3/2019 09:28	47.2	9	0.191	5.4	1.45
2019	4	SNB	ST4300	6/1/2019 14:13	6/3/2019 13:12	47.0	11	0.234	8.4	2.08
2019	5	SNB	ST4300	6/1/2019 15:29	6/3/2019 14:04	46.6	21	0.451	16.5	1.57
2019	6	CB	ST4300	6/1/2019 18:18	6/3/2019 18:18	48.0	6	0.125	3.6	1.50

the sample size of beaked whale acoustic encounters varied among drifts. For some analyses, data are pooled from individual drifts in the same year and location and using the same recorder type (Table II).

A semi-automated approach was used to identify echolocation pulses from Cuvier’s beaked whales (Keating *et al.*, 2018; Simonis *et al.*, 2020) using PAMGuard analysis software (Gillespie *et al.*, 2009). ST4300 recordings at 576 kHz were decimated to yield an effective sampling rate of 288 kHz, and the SM3M recordings were analyzed at their native 256 kHz sampling rate. Impulsive sounds were identified from the digital recordings with an energy detector (the PAMGuard click detector module). The vertical bearing angles to these sound sources (*detection angles*) were automatically calculated in PAMGuard using cross correlation methods. Detection angles are presented here relative to straight down (0°). Impulsive sounds were color-coded based on peak frequency and displayed in the PAMGuard time/bearing display. The PAMGuard Click Template Classifier was also used to highlight impulsive signals that

had a high time-domain correlation with idealized beaked whale pulses. Experienced analysts (Jennifer Keating McCullough, Emily Griffiths, J.S.T., and J.B.) identified signals from Cuvier’s beaked whales based on pulse characteristics and bearing angles (i.e., coming from below the hydrophone array). To avoid false-positive detections (e.g., an isolated echolocation pulse from another species that is similar to that of Cuvier’s beaked whale), a minimum of three beaked whale echolocation pulses within a snapshot (at a consistent bearing angle) were required to qualify as an acoustic detection. Detections with ambiguous species identification or inconsistent bearing angles were excluded from all analyses. Qualitatively, the instrument self-noise was higher for the SM3M recorders than for the ST4300 recorders. Additional details on this analysis approach are provided by Simonis *et al.* (2020).

Foraging dives of beaked whales in a group are highly synchronous (Aguilar de Soto *et al.*, 2018). All the echolocation pulses associated with one foraging dive are referred to as a dive encounter. Analysts identified dive encounters

TABLE II. Acoustic detection parameters for Cuvier’s beaked whales estimated from DASBR drifts pooled by year, location, and recorder type. Locations are detailed in Table I; SNB is the San Nicolas Basin and other basins include the Santa Cruz Basin and Catalina Basin. The mean periods of nearly continuous availability and non-availability are based on periods of detected echolocation pulses without breaks longer than 20 s. Observed dive durations are from the first to the last detected pulse. Effective availability times are estimates from Eq. (7), averaged for snapshot lengths of 10–20 min.

Year	Location	Recorder	Recording duration (h)	No. of dives	Dive detection rate (h ⁻¹)	% minutes with echolocation	Mean period of non-availability (min)	Mean period of availability (min)	Minimum group size	Mean observed encounter duration (min)	Effective availability time (min)
2016	Abyssal north	SM3M	455.9	37	0.081	1.27	2.08	0.52	1.38	21.64	12.28
2016	Abyssal south	SM3M	475.3	19	0.040	0.39	1.80	0.29	1.37	13.22	8.26
2018	SNB	ST4300	119.9	43	0.359	12.61	1.95	1.16	1.98	32.18	26.26
2019	Other basins	ST4300	142.9	23	0.121	3.23	1.68	1.61	1.73	26.12	12.81
2019	SNB	ST4300	93.6	32	0.342	12.03	1.65	1.27	1.74	32.80	19.43
2019	Other basins	SM3M	47.2	9	0.191	5.40	1.83	1.38	1.45	30.56	17.15

by marking associated pulses as “events” within PAMGuard. Echolocation is not expected to occur during the initial portion of their descent or during their final ascent. On average, Cuvier’s beaked whales descend at 1.45 m/s and initiate echolocation at 462 m and ascend at 0.40 m/s and terminate echolocation at 881 m (Barlow *et al.*, 2020; Barlow *et al.*, 2021). Subtracting this estimated silent time (26.3 min comprised of 5.3 min during descent and 21.0 min during ascent) from the mean deep dive duration [65.5 min, standard deviation (s.d.) = 6.4; Barlow *et al.*, 2020] results in an expected mean duration of beaked whale echolocation during a deep foraging dive of 39.2 min. To avoid a biased overestimation of encounter durations caused by dives from two separate groups, temporally associated periods of pulses that were longer than 78 min (twice the mean echolocation period) were sub-divided into two dive encounters, typically at the longest gap without pulses within that period or when detection angles change abruptly.

Echolocation pulses from different individuals within a diving group of beaked whales can often be discerned by differences in bearing angles (Fig. 2). A minimum estimate of group size for each dive encounter was made by counting the maximum number of distinct bearing angles to individual whales that were received at nearly the same time (within a few seconds). The maximum number for an encounter might occur only for a few seconds during the acoustically active phase of a group dive. This count is considered to be a minimum estimate of the number of animals present in a group because it requires all individuals to be detectable at nearly the same time and requires that the angular difference be large enough to be discernible in the PAMGuard bearing/time display. In estimating group size, we assume we are detecting only one diving group during a dive encounter (but see Sec. IV). Empirical data used in this

study include the times and bearing angles of echolocation pulses and the minimum group size for each dive encounter.

B. Fraction of snapshots with acoustic detections

The fraction of snapshots with beaked whale detections (F) is estimated by superimposing snapshot time windows from 20 s to 20 min (20 and 40 s and by 1-min intervals for 1–20 min) on the pulse time series and estimating the fraction of snapshots with at least three beaked whale echolocation pulses. The same distance truncation (6 km) used by Barlow *et al.* (2021) is used here to eliminate distant echolocation pulses. This distance corresponds to a detection angle truncation at 79.9° (the detection angle corresponding to an animal at 6 km horizontal range when it is at an average echolocation depth of 1182 m, i.e., 1072 m below a hydrophone pair at 110 m depth). This angle truncation eliminated 2.4% of Cuvier’s beaked whale echolocation pulses in our sample.

C. Effective area surveyed

We estimate $\hat{\nu}$ from our empirical data for snapshot lengths of 20, 60, 120, 300, 600, and 1200 s (0.33–20.0 min). One mean detection angle is estimated for each snapshot with beaked whale detections. Distance-sampling methods are based on an assumption that horizontal distances (not angles) are unbiased. For group-based estimates, the relevant horizontal distance is to the center of the group. To obtain a mean angle compatible with these expectations, we average the tangents of angles within a snapshot and back-transform this mean tangent to give a mean angle. We use the maximum simulated likelihood approach developed by Barlow *et al.* (2021) to estimate the effective detection radius (EDR) and the effective area surveyed for all drifts pooled. In the simulation portion of this estimation, we use the mean foraging depth distribution for

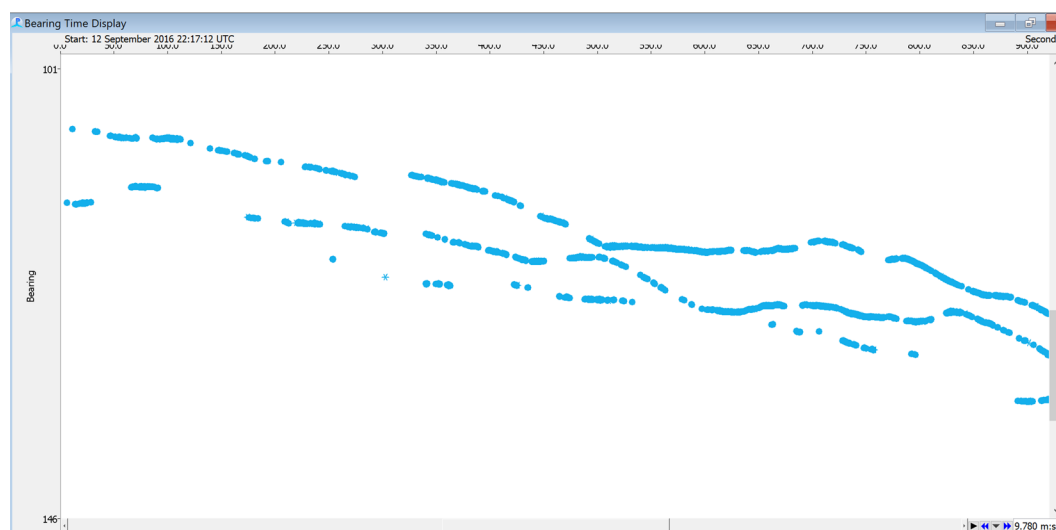


FIG. 2. (Color online) PAMGuard time-bearing display showing the bearing angles (from 101° to 146°) for beaked whale echolocation pulses (blue circles) detected over a 15-min time period. In this example, the minimum group size would be estimated as three based on the minimum number of distinct bearing angles apparent in this display at one time. Due to intermittent availability, the actual number of individuals may be higher. Note that PAMGuard bearing angles are relative to straight up, and the detection angles used in this paper are relative to straight down.

Cuvier’s beaked whales from a tagging study (Barlow *et al.*, 2020) in the same area (mean = 1182 m, s.d. = 305 m). Both the half-normal and compound half-normal detection models are evaluated for an intermediate snapshot length of 5 min, and the best-fit model is chosen based on Akaike’s information criterion (AIC). This detection model is used for all other snapshot lengths. This simulated likelihood method assumes that all echolocating groups are detected at zero absolute distance (slant range) but does not require that all groups be detected at zero horizontal range. EDR is estimated from the estimated detection function, $g(r)$, where r is horizontal range [Eq. (3) in Barlow *et al.* (2021)]. The effective area surveyed, $\hat{\nu}$, is estimated as the area of a circle with this radius.

D. Snapshot availability

The time period of snapshots that potentially contain echolocation signals will be longer than an actual recorded period of echolocation because this time period will typically include time before and after the period of actual acoustic availability. Estimates of snapshot availability [$\hat{\lambda}$ in Eq. (1)] are typically based on the instantaneous probability that an animal is available to be detected. This instantaneous availability, $\hat{\lambda}'$, can be estimated from the time available, t_a , and the time unavailable, t_u , as

$$\hat{\lambda}' = \frac{t_a}{t_a + t_u}.$$

Snapshot availability for a snapshot of duration d can be estimated as

$$\hat{\lambda} = \frac{t_a + d}{t_a + t_u} \quad (3)$$

(McLaren, 1961; Borchers *et al.*, 2013). We estimate $\hat{\lambda}$ using Eq. (3) for the same set of snapshot lengths used to estimate $\hat{\nu}$. The effective acoustic availability time, t_a , is estimated as the mean duration of dive encounters (from the first to the last echolocation pulse) averaged for all dive encounters in the six pooled drifts. Previous studies have used tagging data to estimate acoustic availability time based on observed or predicted times with echolocation (Ward *et al.*, 2012; Barlow *et al.*, 2021). Our effective acoustic availability time is shorter because it excludes times at either the beginning or end of a foraging dive when animals are not oriented toward the hydrophone and are therefore not detectable. Although this definition conflates availability and detectability to some extent, this quantity is empirically measurable with acoustic data and is the appropriate metric to estimate snapshot availability in Eq. (3). The effective time of unavailability, t_u , is estimated as the mean dive period (from the start of one dive to the start of the next dive) for tagged beaked whales in this area (191.4 min; Barlow *et al.*, 2020) minus t_a .

E. Density estimation

To evaluate the effect of snapshot length on resulting estimates of beaked whale density, D , we combine our

snapshot-specific estimates of F , $\hat{\nu}$, and $\hat{\lambda}$ using Eq. (1) to estimate density. For $\hat{\nu}$, we use the average estimate of Cuvier’s beaked whale group size [1.9, coefficient of variation (CV) = 0.07] from visual sighting surveys along the U.S. West Coast (Barlow, 2016).

F. Simulation studies

A computer simulation is used to help understand the range-independent effect of snapshot length on Cuvier’s beaked whale density estimation using acoustic point-transect surveys when animals are not continuously available for detection. Our simulation models the effect of snapshot length on the fraction of snapshots in which acoustic detections occur. Acoustic availability is modeled as a two-part process. Primary availability is the predicted time period over which Cuvier’s beaked whales intermittently produce echolocation pulses; this is parameterized using dive data from tagged whales. Secondary availability characterizes intermittent availability within the period of primary availability, due to such factors as brief pauses in echolocation (Tyack *et al.*, 2006), the orientation of an animal relative to a hydrophone, and the narrow beam width of beaked whale echolocation signals. The secondary availability model is parameterized based on the observed intermittent detection of beaked whales during foraging dives. Snapshot lengths from 20 s to 20 min are modeled. The simulation is written in the R programming language (R Core Team, 2017) with an availability time step of one second (see supplementary material¹ for simulation script in R). In this simulation, detection probability is assumed to be independent of range.

For primary availability, Cuvier’s beaked whales are assumed to produce regular echolocation pulses only during deep foraging dives (Tyack *et al.*, 2006). Primary availability was modeled as a stochastic process with echolocation periods taken with from a normal distribution with a mean of 39.2 min and a CV of 0.15 and a quiet period between echolocation periods taken from a normal distribution with a mean of 152.2 min and a CV of 0.15 [based on a dive period of 191.4 min (Barlow *et al.*, 2020) minus this mean echolocation period of 39.2 min].

Secondary availability within a primary availability window is modeled as a Markov process with two states (available and unavailable). Transitions between states can occur every second based on transition probabilities estimated from observed periods of intermittent availability in our beaked whale acoustic data. The transition probability from available to unavailable is estimated as the inverse of the mean period of nearly continuous availability (“nearly” meaning no gaps longer than the shortest snapshot considered, 20 s). The transition probability from unavailable to available is estimated as the inverse of the mean period of nearly continuous non-availability. Group size is not modeled explicitly in this simulation, but transition probabilities are estimated from our empirical data that contain a distribution of group sizes.

G. Predicted relationship between F and snapshot length

Our simulations are helpful in exploring the effects of snapshot length on the proportion of snapshots with beaked whale detections (F) in a model with primary and secondary availability. However, the effect of snapshot length for the simple case of continuous primary availability can be estimated analytically [Eq. (3)]. Here, we develop a method to estimate the expected relationship between F and the effective availability time (t_a , including the effects of both primary and secondary availability). We treat the acoustic availability time as an unknown and use empirical data to solve for that quantity.

F in Eq. (2) can be re-expressed as the fraction of snapshot times with detections by multiplying the numerator and denominator by the snapshot length, d ,

$$F = \frac{n \cdot d}{k \cdot d}. \tag{4}$$

The expected duration of the snapshots associated with detection i of length t_i is $t_i + d$. If a total of m foraging dives are detected, the numerator above can be re-expressed as

$$n \cdot d = \sum_{i=1}^m (t_i + d)$$

or, equivalently,

$$n \cdot d = m \cdot d + \sum_{i=1}^m t_i. \tag{5}$$

If we define the effective availability time, t_a , as the mean value of acoustic availability time, $\hat{t}_a = (\sum_{i=1}^m t_i) / m$, Eq. (5) becomes

$$n \cdot d = m \cdot (\hat{t}_a + d). \tag{6}$$

From Eq. (6), the effective availability time can be estimated empirically as

$$\hat{t}_a = d \cdot \left[\frac{n}{m} - 1 \right]. \tag{7}$$

Equation (4) can be re-expressed to predict the dependency of F on snapshot duration given an estimate of t_a

$$F = \frac{m \cdot (\hat{t}_a + d)}{k \cdot d}. \tag{8}$$

An empirical estimate of t_a from Eq. (7) (averaged over a range of snapshot lengths from 10 to 20 min) is used with Eq. (8) to estimate F as a function of snapshot length. We compared this expected estimate of F with observed fractions from our empirical and simulation-based studies.

III. RESULTS

A. Empirical studies

A total of 14 drifts in 2016–2019 resulted in 163 detected dive encounters of Cuvier’s beaked whales in the equivalent of 55.6 days of continuous recording effort. The number of echolocation pulses detected per dive encounter was strongly skewed with a long-tailed distribution at higher values (median = 208, mean = 786, and s.d. = 1394). Four of the 163 dive encounters had the minimum number of pulses ($n = 3$) to be included in our analyses. The number of dives per hour and the percentage of 1-min intervals with echolocation signals from Cuvier’s beaked whales varied among drifts (Table I). The highest detection rates were consistently found in the San Nicolas Basin (seven of the eight drifts in that basin were the highest ranking in percentage of minutes with echolocation signals). When drifts are pooled by year, location, and recorder type (Table II), this pattern is even clearer. The two drifts over abyssal waters had the lowest detection rates, and the detection rates in the Santa Cruz Basin and Catalina Basin were intermediate. Minimum group size estimates were also lowest over abyssal waters (Table II). The observed mean durations of dive encounters (the time from the first to the last echolocation pulse in a dive encounter) are longer than the effective availability times estimated from Eq. (7) (Table II).

B. Encounter duration and primary availability

Acoustic encounters are believed to represent a single dive event, often consisting of multiple whales in a synchronously diving group. However, the observed encounter duration averaged for the six pooled drifts (26.1 min) is less than the expected echolocation period during a dive (39.2 min). Encounter durations appear to be dependent on group size, and the encounter duration of larger groups is similar to the expected dive duration (Fig. 3). Mean encounter durations were longest for drifts in the San Nicolas Basin, which also had the greatest estimates of minimum group size (Table II).

The period of primary availability is defined as the echolocation portion of a deep foraging dive. Because the mean encounter duration is less than the expected echolocation period, we use the former to estimate instantaneous and snapshot availabilities (Table III).

C. Density estimation

The three terms we examined in the density estimation equation (F , $\hat{\nu}$, and $\hat{\lambda}$) were all found to increase with snapshot length (Table III). The fraction of snapshots with detections of Cuvier’s beaked whales, F , increases rapidly with snapshot length from 20 s to 5 min (Fig. 4). For snapshot lengths greater than 10 min, this increase appears to be linear and is well approximated by the relationship predicted by Eq. (8) [using estimates of effective availability time, \hat{t}_a , from Eq. (7)] (Table II). Mean detection angles for echolocation pulses (within the truncation angle) increase with snapshot length up to about 10 min (Fig. 5). For the

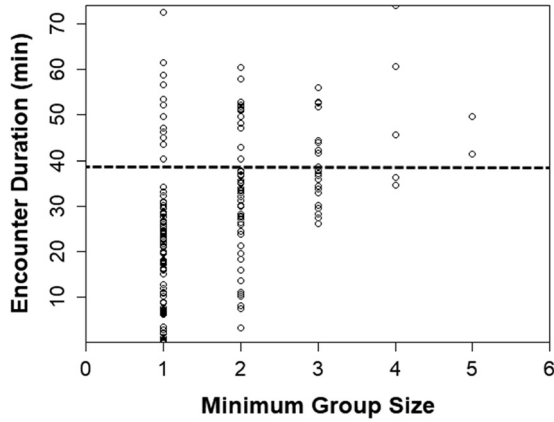


FIG. 3. Observed encounter durations as a function of minimum group size. The horizontal dashed line represents the expected duration of echolocation during a foraging dive (39.2 min).

distance-sampling estimates of detection probability with distance, the half-normal detection model for 5-min snapshots was selected based on having a lower value of AIC ($\Delta AIC = 1.23$) and a Kolmogorov–Smirnov (K–S) goodness of fit ($p = 0.997$) similar to that of the compound half-normal model ($p = 0.969$). Estimated detection functions for the half-normal model are illustrated in Fig. 6. As expected, given the increase in mean detection angles, effective detection radii and effective areas surveyed for the half-normal model increase with snapshot length (Table III). Estimates of snapshot availability also increased with snapshot length (Table III), as expected from Eq. (3).

Overall, snapshot length has very little effect on estimated densities (Table III) due to the compensatory effects of increases in both the numerator and denominator of Eq. (1). Although the shortest (20 s) and longest (20 min) snapshots yielded the lowest and highest density estimates, respectively, all estimates are comparable, with an overall mean value of 34.3 (s.d. = 1.9) whales/1000 km².

D. Simulation results

For the simple simulations with primary availability only, the fraction of snapshots with acoustic detections increases linearly with snapshot length (Fig. 7). The estimated effective availability time, t_a , from that simulation (39.0 min) is in good agreement with the mean echolocation time used to generate the simulated data (39.2 min). Likewise, the predicted fraction of snapshots with acoustic

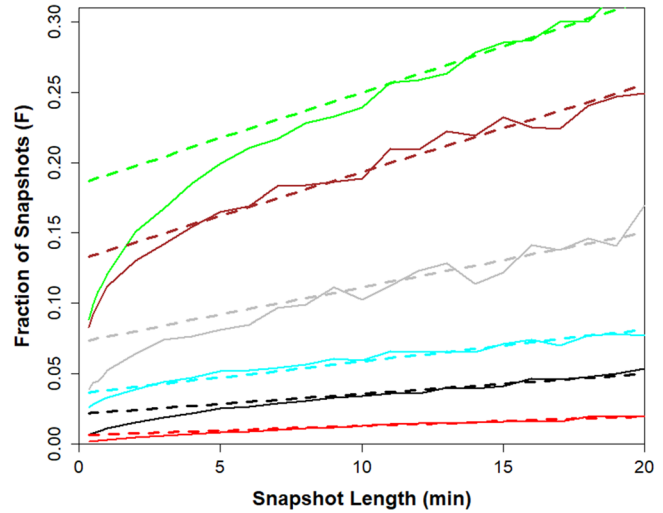


FIG. 4. (Color online) Observed fractions of snapshots with beaked whale acoustic detections (F , solid lines) as a function of snapshot length for pooled drifts. The dashed lines show the expected relationship calculated by Eq. (8) using the estimated effective availability times for the given drifts (Table II). Lines are color-coded by pooled drift (2016 in red and black; 2018 in green; and 2019 in cyan, brown, and gray).

detections is in good agreement with the simulated values (Fig. 7) over the full range of snapshot lengths.

For the simulations with both primary and secondary availability, the Markov transition probabilities for intermittent secondary availability within the window of primary availability are estimated from the empirical data from the pooled drifts (Table II). Within dive encounters, periods without gaps in echolocation pulses longer than 20 s (the shortest snapshot length considered here) averaged 62.2 s. Periods of silence longer than 20 s and shorter than 20 min averaged 109.7 s. Using the inverse of these mean values as Markov transition probabilities (per second) for transition between available and unavailable states, the simulated fraction of snapshots with detections increases rapidly with snapshot length from 20 s to 5 min and increases linearly with snapshot lengths longer than ~ 7 min (Fig. 7). The effective availability time is estimated to be 36.6 min. Using this latter value for t_a , Eq. (8) accurately predicts the simulated values of F for snapshot lengths greater than 7 min for simulations with intermittent secondary availability. Simulated values of F are 3.5% and 33.8% less than the predicted values for snapshot lengths of 5 and 1 min, respectively.

TABLE III. Effects of snapshot duration on estimates of the fraction of snapshots with detections (F), the EDR, the effective area surveyed (A), snapshot availability ($\hat{\lambda}$), and whale density (D). Estimates of instantaneous availability ($\hat{\lambda}'$) and mean group size (s) are the same for all snapshot lengths.

Snapshot duration (min)	F	EDR (km)	A (km ²)	$\hat{\lambda}'$	$\hat{\lambda}$	s	D (individuals/1000 km ⁻²)
0.33	0.040	2.36	17.5	0.136	0.138	1.9	31.7
1	0.055	2.59	21.0	0.136	0.142	1.9	35.2
2	0.067	2.87	25.8	0.136	0.147	1.9	33.7
5	0.088	3.02	28.6	0.136	0.162	1.9	36.1
10	0.106	3.23	32.7	0.136	0.189	1.9	32.7
20	0.148	3.19	32.0	0.136	0.241	1.9	36.4

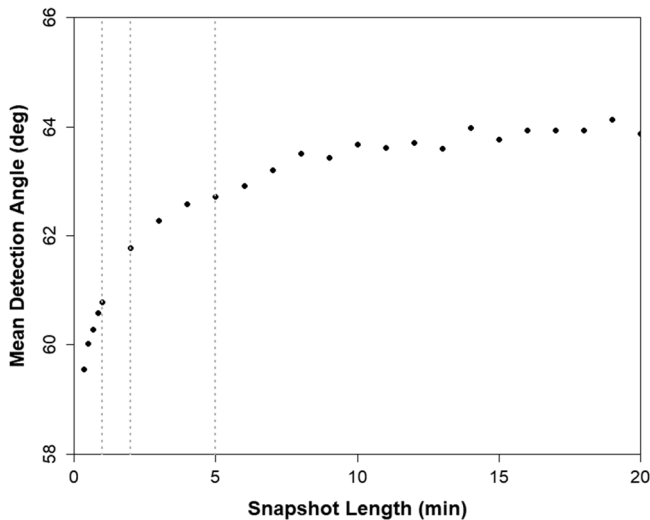


FIG. 5. Empirical relationship between snapshot length and mean detection angle for snapshot lengths of 20 s to 20 min. Vertical dotted lines represent snapshot lengths of 1, 2, and 5 min.

IV. DISCUSSION

A. Snapshot length

The selection of snapshot length in point-transect surveys involves a trade-off between meeting two important assumptions: (1) that all individuals or groups can be detected if they are very close to the sampling point (or that the fraction missed can be estimated) and (2) that animal or group movement during a snapshot is trivially small. Variable length snapshots were superimposed on continuous recordings from 14 DASBR drifts off central and southern California. Results show that the fraction of snapshots with acoustic detections of Cuvier’s beaked whales, F , increases with snapshot lengths, particularly for snapshots less than 5 min. Our simulation study shows that primary availability alone should result in a linear increase in F with snapshot length, whereas realistic levels of secondary availability can explain the rapid falloff in F at values below 5 min. However, estimates of effective area surveyed and effective

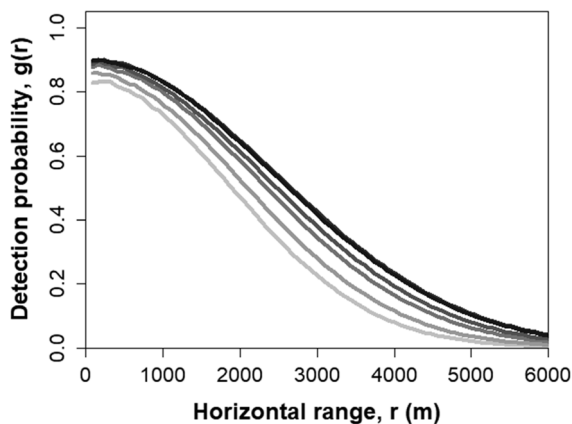


FIG. 6. Estimated detection functions for snapshot lengths of 0.33, 1, 2, 5, 10, and 20 min, respectively (from light gray to black). Estimates for 10 and 20 min are superimposed and indistinguishable on this scale.

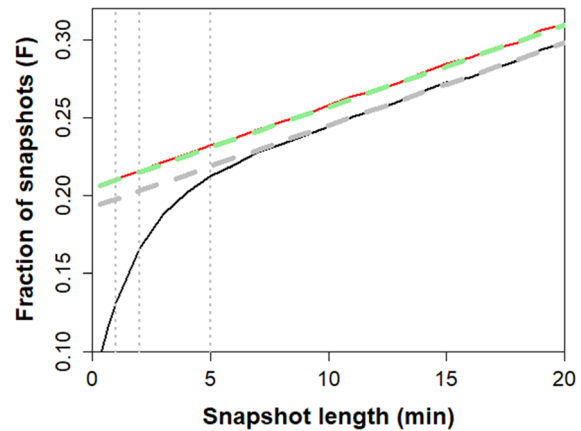


FIG. 7. (Color online) Simulation-based estimates of the fractions of snapshots with beaked whale acoustic detections (F) as a function of snapshot length. Simulation results include primary availability only (red line) and primary plus secondary availability (black line). The green and gray dashed lines, respectively, show the expected relationship predicted by Eq. (8) using the estimated effective availability times from those simulations. Vertical dotted lines represent snapshot lengths of 1, 2, and 5 min. For the simulation with both primary and secondary availability, these correspond to reductions of 33.8%, 18.6%, and 3.5%, respectively, relative to the expected values (gray dashed line).

snapshot availability also increase with snapshot length and compensate for changes in F when making estimates of whale density. The increase in effective area surveyed with snapshot length is likely the result of distant detections being more intermittent. Intermittent detections are more likely to be missed if snapshot lengths are short. Given the other sources of uncertainty in estimating density, snapshot lengths from 20 s to 20 min give roughly equivalent estimates of density (mean = 34.3 whales/1000 km²).

Based on our results, we recommend snapshot lengths of 1–2 min for acoustic point-transect surveys of Cuvier’s beaked whales. This range of time periods allows for a relatively high probability of detecting groups that are present within the acoustic detection range of a drifting hydrophone recorder. Short snapshots are desirable to minimize movement during a snapshot and to increase the sample size of snapshots for precisely estimating the fraction of snapshots with detections and the effective area surveyed. However, our shortest snapshot length (20 s) yielded a density estimate that was lower than any other, and we would recommend additional studies before selecting such a short interval. There appears to be little benefit of increasing the snapshot length above 5 min because, above this value, the increase in the fraction of positive detections is entirely explained by the mechanistic effect of snapshot length [per Eq. (8)] and appears to be unrelated to an actual increase in detection probability.

For longer-term studies (e.g., multi-day drifts), recordings from drifting hydrophones might be duty cycled to achieve a greater geographic coverage from systems with limited memory or battery life (Keating *et al.*, 2018; Simonis *et al.*, 2020). Our method of sub-setting continuous recordings would not be directly applicable for duty-cycled recordings. However, information from this study with

continuous recordings may help inform the choice of duty cycles for longer-term recordings with limited memory or battery life. For example, a duty cycle with 1-min recordings would result in twice the number of snapshots as 2-min recordings, which could be used to extend recording durations and geographic coverage for drifting recording systems.

We did not specifically examine the effect of snapshot length on variance estimation, in part because our method of sub-setting continuous recordings results in temporal auto-correlation in snapshot samples. To realistically estimate the potential benefit of shorter snapshots in reducing the variance of density estimates (by increasing sample size) would require duty sampled recordings. Overall, we expect that the larger sample size obtained by using shorter snapshots would reduce the variance in estimating the detection function but that the reduction in auto-correlation from duty cycling might result in higher (albeit more realistic) variance estimates.

B. Availability time

Estimates of effective availability time are much less than our observed encounter durations (Table II), which are less than the expected duration of the echolocation period of foraging dives (estimated from tagged animals). We introduce the term primary availability to describe the period when animals are producing echolocation pulses and are potentially available to be detected. We use the term secondary availability to describe the times within this primary availability window when animals are oriented so that their echolocation signals can actually be detected by a hydrophone recorder. Gaps in detection can be caused by changes in orientation relative to the hydrophone and other details of their foraging behavior. The echolocation pulse of Cuvier's beaked whales is narrow, with a 3 dB beam width of only 6° (Zimmer *et al.*, 2005), so even small changes in orientation can greatly affect whether a whale is detectable. Given this intermittent secondary availability, shorter snapshots are more likely to miss potential detections. Intermittent availability also explains why observed encounter durations are expected to be shorter than the period of echolocation during a dive. Whales may not be available for detection at the start or end of an echolocation period.

Because secondary availability is dependent on animal behavior, secondary availability may differ among study areas. Tracking studies of Cuvier's beaked whales (Gassmann *et al.*, 2015; Aguilar de Soto *et al.*, 2018; Barlow *et al.*, 2018) show that large changes in direction are common during a foraging dive. Periods of non-availability are likely to be shorter if foraging animals are turning more rapidly. In areas with small patches of good foraging habitat, whales might be expected to turn more rapidly, thereby remaining within those small patches. Caution should be used when using estimates of availability from one area in another.

Our concept of secondary availability could be more simply viewed as missed detections in a distance-sampling framework. Detections could be missed within a period of primary availability due to brief pauses in nearly continuous periods of echolocation, due to range-independent factors such as animal orientation (as discussed above), and due to range-dependent factors that are expected to decrease detection probability with range. In our formulation, the range-dependent effect is incorporated into the estimation of effective area surveyed. The former two effects on detection probability could be incorporated into a $g(0)$ term that typically represents the probability of detection at zero horizontal distance. We distinguish between the effects of what we call secondary availability and our $g(0)$ term, which describes the detection probability at zero horizontal distance caused by an animal's depth (because our formulation for detection probability is based on slant range, which, at zero horizontal distance, is equal to depth below the hydrophone). Although we recognize that this distinction between secondary availability and $g(0)$ is somewhat arbitrary, we find it useful.

Effective availability time (estimated as a mean value for snapshot lengths of 10–20 min) is useful in predicting the expected relationship between the fraction F of snapshots with detections and snapshot length but may have no useful meaning outside that context. Effective availability times are likely to be shorter than the potential period of primary availability (when whales are echolocating) because of intermittent availability. The difference between effective availability time and dive foraging time was much smaller for our simulation study, likely because our simple simulation did not include the effects of orientation relative to the hydrophone on detection probability.

C. Minimum group size

We estimate minimum group size as the maximum number of distinct bearing tracks detected during an acoustic encounter. The mean estimate for all drifts (1.83, from Table I) is slightly less than the mean group size estimate of 1.9 from visual sighting surveys off the U.S. West Coast. Because the former is based on minimum counts, we used the latter in our density estimates (Table III); however, this difference is trivially small. Marques *et al.* (2019) developed an acoustic method of estimating beaked whale group sizes based on the “acoustic footprint.” That method uses visually validated group sizes in a regression model that estimates group size from the total number of echolocation pulses detected on an array of bottom-mounted hydrophones. The Marques *et al.* (2019) approach should produce unbiased estimates of group size but is not readily applicable to single-point acoustic surveys. Hildebrand *et al.* (2015) estimated beaked whale group sizes from the regular patterns of intervals between echolocation pulses and patterns of changing amplitude. That method is likely to also produce a minimum estimate if all individuals in a group are not detectable at the same time; however, it produced mean estimates of

Cuvier's beaked whale group size (1.95) that are also similar to estimates from visual sighting surveys. A combination of our method using bearing angles and the method of Hildebrand *et al.* (2015) using inter-pulse-intervals might be able to provide more robust estimates of group size for single-point surveys than either method used separately.

Our highest estimates of minimum group size are in the San Nicolas Basin, and our lowest estimates are in the two drifts over the abyssal plain. This may represent a real difference or may be caused by the shorter encounter durations over the abyssal plain (Table II). Acoustic methods may underestimate group size when encounter durations are short because all individuals are less likely to be detectable at the same time. Conversely, encounter durations may be shorter for smaller groups because the true start and end times of a dive are more likely to be missed. However, Curtis *et al.* (2020) report a mean group size of 3.0 (s.d. = 1.8) from photo-identification studies in the San Nicolas Basin, which suggests that our larger group sizes there may represent a real difference.

D. Simultaneous detection of multiple groups

We assumed that only one group was acoustically detectable at one time. This assumption is easily met in low density areas, such as during our abyssal drifts, when less than 2% of minutes had detections of Cuvier's beaked whales (Table I). However, in higher density areas of the San Nicolas Basin, beaked whales were detected during 8%–18% of minutes. With such high detection rates, multiple beaked whale groups are likely to be occasionally detected at the same time, particularly if groups aggregate in good foraging areas. Our assumption would treat multiple groups as a single group (with an average group size of 1.9) and thus would underestimate whale density in high-density areas. The higher minimum group sizes in the San Nicolas Basin could have resulted from counting multiple simultaneously detected groups as a single group.

E. Detection function

For all snapshot durations, our estimated probabilities of detection were between 0.82 and 0.9 at zero horizontal distance (Fig. 6). Our estimated probabilities of detection at 4 km are higher than have been previously estimated from propagation models. Propagation models may underestimate detection range if they are based only on the center frequency of echolocation pulses [40 kHz in Zimmer *et al.* (2008)] rather than on the full bandwidth of signals (Ainslie, 2013; von Benda-Beckmann *et al.*, 2018). Some of our more distant detections had peak frequencies of 18–22 kHz. The lower-frequency components of Cuvier's beaked whale echolocation pulses are subject to less propagation loss and appear to extend the range at which these pulses can be detected.

Our estimates of EDR increase with snapshot duration up to a maximum for 10-min snapshots. Our estimate for a 1-min snapshot (2.6 km) is less than the distance-sampling

estimate of Barlow *et al.* (2021) for 1-min snapshots (3.0 km) in the Catalina Basin. That study found that a compound half-normal detection function gave a better fit than a half-normal model with the same truncation distance. The greater EDR and different detection function in the Catalina Basin may be related to its depth (~1250 m), which is shallower than any of the other areas in our study. For a given horizontal distance, whales are likely to be more detectable at shallower depths because the absolute distance to a near-surface hydrophone is less. Based on a propagation modeling approach, Hildebrand *et al.* (2015) estimate that the mean probability of detecting a group of Cuvier's beaked whales within a radius of 4 km of a bottom-moored recorder in a 5-min snapshot is 0.359, which corresponds to an EDR of 2.4 km. This is less than our EDR estimate of 3.0 km for 5-min snapshots, but these estimates are not directly comparable due to the different truncation distances.

F. Density estimates

Our estimates of density for Cuvier's beaked whales (~34 whales/1000 km²; Table III) are among the highest values ever estimated for this species. Barlow (2006) estimated a density of 6.2 whales/1000 km² from a visual sighting survey in the Hawaiian economic zone (EEZ). The average estimate for seven visual sighting surveys in EEZ waters off the U.S. West Coast is 3.2 whales/1000 km² (Barlow, 2016). Hildebrand *et al.* (2015) estimated 0.3–16 whales/1000 km² using two acoustic density estimation methods at three sites in the Gulf of Mexico. The highest density estimate from a visual sighting survey is 38 whales/1000 km² in the southern Gulf of California, Mexico (Ferguson and Barlow, 2001). Within our study area, Falcone *et al.* (2009) estimated a minimum density of 50 whales/1000 km² based on the photo-identification of 21 unique Cuvier's beaked whales in the San Nicolas Basin within a 4-day period in 2007. However, it is important to note that the percentage of minutes with detections in our study varied by more than an order of magnitude from mean values of 0.8% over abyssal plains to 12.3% in the San Nicolas Basin. This basin appears to have an extraordinarily high density of Cuvier's beaked whales, and the high density estimate from this study is strongly weighted by the high level of survey effort there. A meaningful density estimate for any of these study areas would require a more systematic sampling design that representatively covered a defined study area.

ACKNOWLEDGMENTS

We are grateful to all who helped with the collection and analysis of the data used in this report. Annette Henry coordinated the 2016 field work. Jennifer Keating McCullough and Emily Griffiths analyzed the beaked whale detections from 2016. Brenda Rone aided in field data collection in 2018, with additional support provided by the Marine Mammal Monitoring on Navy Ranges (M3R) group from the Naval Undersea Warfare Center. Anne Simonis

and Taiki Sakai aided in data collection in 2019. We thank the offices and crew aboard the research vessels Shimada and New Horizon for their help in collecting these data. Funding was provided by the U.S. Navy's Living Marine Resources Program, the U.S. Navy's Pacific Fleet, the U.S. Bureau of Ocean Energy Management (BOEM), National Oceanic and Atmospheric Administration (NOAA)'s Southwest Fisheries Science Center, and NOAA's Cooperative Research Program. Len Thomas, Tiago Marques and Erin Oleson provided helpful comments on an earlier version of this manuscript.

¹See supplementary material at <https://www.scitation.org/doi/suppl/10.1121/10.0005108> for R code simulation of the effect of snapshot length and intermittent availability on the estimation of the fraction of snapshots with beaked whale acoustic detections.

- Aguilar de Soto, N., Visser, F., Madsen, P. T., Tyack, P., Ruxton, G., Alcazar, J., Arranz, P., and Johnson, M. (2018). "Beaked and killer whales show how collective prey behaviour foils acoustic predators," *BioRxiv*:303743.
- Ainslie, M. A. (2013). "Neglect of bandwidth of Odontocetes echo location clicks biases propagation loss and single hydrophone population estimates," *J. Acoust. Soc. Am.* **134**, 3506–3512.
- Barlow, J. (2016). "Cetacean abundance in the California Current estimated from ship-based line-transect surveys in 1991–2014," in *NOAA Southwest Fisheries Science Center Administrative Report LJ-16-01, Southwest Fisheries Science Center, La Jolla, CA*.
- Barlow, J. (2006). "Cetacean abundance in Hawaiian waters estimated from a summer/fall survey in 2002," *Mar. Mamm. Sci.* **22**, 446–464.
- Barlow, J., Fregosi, S., Thomas, L., Harris, D., and Griffiths, E. T. (2021). "Acoustic detection range and population density of Cuvier's beaked whales estimated from near-surface hydrophones," *J. Acoust. Soc. Am.* **149**, 111–124.
- Barlow, J., Griffiths, E. T., Klinck, H., and Harris, D. V. (2018). "Diving behavior of Cuvier's beaked whales inferred from three-dimensional acoustic localization and tracking using a nested array of drifting hydrophone recorders," *J. Acoust. Soc. Am.* **144**, 2030–2041.
- Barlow, J., Schorr, G., Falcone, E., and Moretti, D. (2020). "Variation in dive behavior of Cuvier's beaked whales with seafloor depth, time-of-day, and lunar illumination," *Mar. Ecol. Progr. Ser.* **644**, 199–214.
- Barlow, J., Tyack, P. L., Johnson, M. P., Baird, R. W., Schorr, G. S., Andrews, R. D., and Aguilar de Soto, N. (2013). "Trackline and point detection probabilities for acoustic surveys of Cuvier's and Blainville's beaked whales," *J. Acoust. Soc. Am.* **134**, 2486–2496.
- Baumann-Pickering, S., McDonald, M. A., Simonis, A. E., Solsona Berga, A., Merckens, K. P. B., Oleson, E. M., Roch, M. A., Wiggins, S. M., Rankin, S., Yack, T. M., and Hildebrand, J. A. (2013). "Species-specific beaked whale echolocation signals," *J. Acoust. Soc. Am.* **134**, 2293–2301.
- Borchers, D. L., Zucchini, W., Heide-Jørgensen, M. P., Cañadas, A., and Langrock, R. (2013). "Using hidden Markov models to deal with availability bias on line transect surveys," *Biometrics* **69**(3), 703–713.
- Buckland, S. T. (2006). "Point-transect surveys for songbirds: Robust methodologies," *Auk* **123**, 345–357.
- Curtis, K. A., Falcone, E. A., Schorr, G. S., Moore, J. E., Moretti, D. J., Barlow, J., and Keene, E. (2020). "Abundance, survival, and annual rate of change of Cuvier's beaked whales (*Ziphius cavirostris*) on a Navy sonar range," *Mar. Mamm. Sci.* **37**, 399–419.
- Falcone, E., Schorr, G. S., Douglas, A., Calambokidis, J., Henderson, E., McKenna, M., Hildebrand, J., and Moretti, D. (2009). "Sighting characteristics and photo-identification of Cuvier's beaked whales (*Ziphius cavirostris*) near San Clemente Island, California: A key area for beaked whales and the military?" *Mar. Biol.* **156**, 2631–2640.
- Ferguson, M. C., and Barlow, J. (2001). "Spatial distribution and density of cetaceans in the eastern tropical Pacific Ocean based on summer/fall research vessel surveys in 1986–96," SWFSC Administrative Report No. LJ-01-04, Southwest Fisheries Science Center, La Jolla, CA.
- Gassmann, M., Wiggins, S. M., and Hildebrand, J. A. (2015). "Three-dimensional tracking of Cuvier's beaked whales' echolocation sounds using nested hydrophone arrays," *J. Acoust. Soc. Am.* **138**, 2483–2494.
- Gillespie, D., Mellinger, D. K., Gordon, J., McLaren, D., Redmond, P., McHugh, R., Trinder, P., Deng, X.-Y., and Thode, A. (2009). "PAMGUARD: Semiautomated, open source software for real-time acoustic detection and localization of cetaceans," *J. Acoust. Soc. Am.* **125**, 2547.
- Glennie, R., Buckland, S. T., Langrock, R., Gerrodette, T., Ballance, L. T., Chivers, S. J., and Scott, M. D. (2020). "Incorporating animal movement into distance sampling," *J. Am. Stat. Assoc.* **116**, 107–115.
- Hildebrand, J. A., Baumann-Pickering, S., Frasier, K. E., Trickey, J. S., Merckens, K. P., Wiggins, S. M., McDonald, M. A., Garrison, L. P., Harris, D., Marques, T. A., and Thomas, L. (2015). "Passive acoustic monitoring of beaked whale densities in the Gulf of Mexico," *Sci. Rep.* **5**, 15.
- Keating, J. L., Barlow, J., Griffiths, E. T., and Moore, J. E. (2018). "Passive acoustics survey of cetacean abundance levels (PASCAL-2016) final report," OCS Study BOEM 2018-025, Department of the Interior, Bureau of Ocean Energy Management, Honolulu, HI.
- Lee, D. C., and Marsden, S. J. (2008). "Adjusting count period strategies to improve the accuracy of forest bird abundance estimates from point transect distance sampling surveys," *Ibis* **150**(2), 315–325.
- Marques, T. A., Jorge, P. A., Mourinho, H., Thomas, L., Moretti, D. J., Dolan, K., Claridge, D., and Dunn, C. (2019). "Estimating group size from acoustic footprint to improve Blainville's beaked whale abundance estimation," *Appl. Acoust.* **156**, 434–439.
- Marques, T. A., Thomas, L., Martin, S. W., Mellinger, D. K., Ward, J. A., Moretti, D. J., Harris, D., and Tyack, P. (2013). "Estimating animal population density using passive acoustics," *Biol. Rev.* **88**, 287–309.
- McLaren, I. A. (1961). "Methods of determining the numbers and availability of ring seals in the Eastern Canadian Arctic," *Arctic* **14**, 162–175.
- R Core Team (2017). "R: A language and environment for statistical computing," R Foundation for Statistical Computing, Vienna, Austria.
- Schorr, G. S., Falcone, E. A., Moretti, D. J., and Andrews, R. D. (2014). "First long-term behavioral records from Cuvier's beaked whales (*Ziphius cavirostris*) reveal record-breaking dives," *PLoS One* **9**, e92633.
- Simonis, A. E., Trickey, J. S., Barlow, J., Rankin, S., Urbán, J., Rojas-Bracho, L., and Moore, J. E. (2020). "Passive acoustics survey of Odontocetes in the California Current ecosystem 2018: Final report," NOAA technical memorandum NMFS-SWFSC-630, National Oceanic and Atmospheric Administration, Washington, DC.
- Tyack, P. L., Johnson, M., Aguilar Soto, N., Sturlese, A., and Madsen, P. T. (2006). "Extreme diving of beaked whales," *J. Exp. Biol.* **209**, 4238–4253.
- von Benda-Beckmann, A. M., Thomas, L., Tyack, P. L., and Ainslie, M. A. (2018). "Modelling the broadband propagation of marine mammal echolocation clicks for click-based population density estimates," *J. Acoust. Soc. Am.* **143**, 954–967.
- Ward, J. A., Thomas, L., Jarvis, S., DiMarzio, N., Moretti, D., Marques, T. A., Dunn, C., Claridge, D., Hartvig, E., and Tyack, P. (2012). "Passive acoustic density estimation of sperm whales in the Tongue of the Ocean, Bahamas," *Mar. Mamm. Sci.* **28**, E444–E455.
- Warren, V. E., Marques, T. A., Harris, D., Thomas, L., Tyack, P. L., Aguilar de Soto, N., Hickmott, L. S., and Johnson, M. P. (2017). "Spatio-temporal variation in click production rates of beaked whales: Implications for passive acoustic density estimation," *J. Acoust. Soc. Am.* **141**, 1962–1974.
- Zimmer, W. M. X., Harwood, J., Tyack, P. L., Johnson, M. P., and Madsen, P. T. (2008). "Passive acoustic detection of deep-diving beaked whales," *J. Acoust. Soc. Am.* **124**, 2823–2832.
- Zimmer, W. M. X., Johnson, M. P., Madsen, P. T., and Tyack, P. L. (2005). "Echolocation clicks of free-ranging Cuvier's beaked whales (*Ziphius cavirostris*)," *J. Acoust. Soc. Am.* **117**, 3919–3927.